Preparation of Polymeric Micelles of Poly(Ethylene Oxide-b-Lactic Acid) and their Encapsulation With Lavender Oil

Tatiane Popiolski, Issei Otsuka, Sami Halila, Edvani Muniz, Valdir Soldi, Redouane Borsali

Materials Research. 2016; 19(6): 1356-1365
DOI: http://dx.doi.org/10.1590/1980-5373-MR-2016-0430

Preparation of Polymeric Micelles of Poly(Ethylene Oxide-*b*-Lactic Acid) and their Encapsulation With Lavender Oil

Tatiane M. Popiolski[a,b], Issei Otsuka[a], Sami Halila[a], Edvani C. Muniz[c], Valdir Soldi[b,d]*, Redouane Borsali[a]

[a] *Centre de Recherches sur les Macromolécules Végétales, CERMAV, UPR-CNRS 5301, Grenoble, Cedex 9, France*

[b] *Departamento de Engenharia e Ciência dos Materiais, Departamento de Química, Universidade Federal de Santa Catarina,CEP 88040-900 , Florianopolis, SC, Brazil*

[c] *Grupo de Materiais Poliméricos e Compósitos, GMPC—Departamento de Química, Universidade Estadual de Maringá, CEP 87020-900, Maringá, PR, Brazil*

[d] *Instituto Brasileiro de Tecnologia do Couro, Calçado e Artefatos-IBTeC, CEP 93334-000, Novo Hamburgo, RS, Brazil*

Received: June 06, 2016; Revised: August 10, 2016; Accepted: September 07, 2016

Nanoparticles comprised of the poly(ethylene oxide)-*b*-poly (lactic acid) diblock copolymer (PEO-*b*-PLA) with and without the incorporation of lavender oil were prepared by nanoprecipitation. Diblock copolymers based on a fixed PEO block (5_{KDa}) and two different PLA segments (4.5 or 10_{KDa}) were used. The morphology, encapsulation efficiency, essential oil-polymer interaction and the release kinetics of the active agent in the nanoparticles, were evaluated. The hydrodynamic radius of the nanoparticles determined by light scattering was affected by the size of the poly(lactic acid) (PLA) block. The lavender essential oil encapsulation efficiency (at a concentration of 0.4 μL mL^{-1}) determined by UV-VIS spectroscopy was in the range of 70-75%. The in vitro release suggests that the polymeric barrier is able to control the oil release.

Keywords: *block copolymer, nanoparticles, morphology, lavender oil.*

1. Introduction

Interest in the self-assembly of block copolymer systems has been growing and is today one of the most important fields of nanotechnology.[1] Micelles obtained from block copolymers play an important role in the delivery of active substances, particularly for water-insoluble molecules.[2] The development of nanoparticles has been characterized as a promising strategy for different applications, for instance, the incorporation, transport and release of active substances, such as drugs, oils and essences.[3-6]

Poly(lactic acid) (PLA) is a biodegradable and biocompatible polyester widely used in applications related to the area of medicine.[7] For example, PLA and its copolymers have been used in tissue engineering for the restoration of impaired tissues and also in the development of nanoparticles for drug delivery.[8,9]

Poly(ethylene oxide) (PEO) is also non toxic and does not show antigenicity and immunogenicity. However, as PEO is non biodegradable and exhibits extraordinarily large hydrodynamic volume. This fact limits the use of high molecular weight analogues of PEO to health.

One of the most interesting systems is the block copolymer comprised of PLA-*b*-PEO, which is able to form thermodynamically stable nanoparticles through a self-assembly process.[10,11] Dai and Lim demonstrate the feasibility of entrapping mustard seed meal powder particles in nonwovens produced by electrospinning PLA-*b*-PEO blends into ultrafine fibers, as an antibacterial agent for controlled release.[12]

Jie et al used the PEO-*b*-PLA copolymers to compare the kinetics of drug release for star-branched, tri- and di-block copolymers. The drug release profile showed that the release of paclitaxel from these polymers could be controlled over weeks. Also, the lower hydrodynamic radius of star-shaped polymers may result in better clearance of the carrier polymer from the body.[13] A family of strong, highly flexible biodegradable polymers was developed, by capitalizing on the particular morphology and superior mechanical properties and PEO-*b*-PLA are one of the copolymers which displaying their enhanced mechanical properties.[14] Random and block copolymers of lactic acid with glycolic acids, ε-caprolactone and poly(ethylene glycol) (PEG) are commonly used as drug carriers.[15]

Studies on the encapsulation and controlled-release of the common anticancer agent doxorubicin, in vesicles obtained from hydrolysable diblock copolymers of (PEG-*b*-PLA) and poly(ethylene glycol)–poly(caprolactone) (PEG-*b*-PCL), have been reported.[16] The authors demonstrated that the rate of doxorubicin release from the hydrolysable vesicles is accelerated with an increased proportion of PEG, but decreased with a more hydrophobic chain chemistry. Riley et al. (2001) reported similar studies using nanoparticles obtained from PEG-*b*-PLA with a fixed PEG block (5 KDa) and varying the PLA segment (2-110 KDa).[17]

* e-mail: soldi.valdir@gmail.com

Essential oils generally, are volatile substances, sensitive to oxygen, light, moisture, and heat. These reported special characteristics could diminish their applicability in the use of cosmetics, food, products pharmaceutical and industries. Thus, encapsulation and particularly, nanoencapsulation, is one of the most efficient methods for the formulation of active substances, being a viable and efficient approach to increasing its physical stability and protecting them from interactions with environmental factors, such as, pH, oxygen, light and moisture.[18-20] For example, solid lipid microparticles (SLM) were used to encapsulate juniper oil, in order to reduce the volatility of the antimicrobial agent, applied to treatment of acne vulgare.[21] The encapsulation of eugenol and carvacrol into nanometric surfactant micelles for the solubilization in the aqueous phase also resulted in enhanced antimicrobial activity against two pathogenic bacteria.[22] The encapsulation of terpenes mixture extracted from Melaleuca alternifolia and D-limonene, was used as a method to improve the safety and quality of foods through the addition of natural preservatives, in order to increase and retain the antimicrobial activity of the encapsulated compounds. The formulations were tested in fruit juices, in order to evaluate it preservation from inoculated spoilage microorganisms and shelf life extension against the alteration of the quality parameters.[20]

Lavender oil (LO), which has antifungal and antibacterial properties and acts as a sedative, antiseptic and analgesic,[23,24] is also used for their pleasant scent, was used in this study. Lavender oil was encapsulated in gum arabic and compared with to gelatin. The authors reported one encapsulation efficiency of 66%, the appearance of microcapsules is sphere and the surface is smooth without aggregation.[19] The incorporation of the natural products, in the form of oil eliminates the need for precursor preparation. Balasubramanian et al., utilized the lavender oil fabricated in an electrospun PAN nanofiber for antibacterial and drug delivery applications. Moreover, these nanofibers can be fabricated to advanced morphologies like porous, core and shell nanofibers carrying encapsulations and sandwich morphologies using various antimicrobial additives to enhance the sustained drug release and antimicrobial property.[25]

The original contribution of this work was the encapsulation of lavender essential oil in nanostructured systems (nanoparticles), developed for application as antibacterial agent in textiles components used in the footwear industry. Lavender oil was encapsulated in nanoparticles prepared from the diblock copolymer (PEO-*b*-PLA), aimed at slowing the volatilization of volatile cores and protecting the active agent from unwanted interactions with the external environment. This copolymer has self-association properties in aqueous medium and is able to form thermodynamically stable colloidal suspensions. The nanoparticles were prepared by the nanoprecipitation technique, as described by Fessi et al.,[26] and parameters such as the size, morphology, zeta potential, encapsulation and release profile for lavender oil in this system were evaluate.

2. Experimental

2.1. Materials

The diblock copolymers PEO_{5kDa}-*b*-$PLA_{4.5kDa}$ and PEO_{5kDa}-*b*-PLA_{10kDa} used in this study were purchased from Polymer SourceTM (Montreal, Canada). Acetone (Carlo Erba) and water (purified in a Milli-Q water purification system; Billerica, MA, USA) were used to prepare the nanoparticles. The lavender oil, which was used as an active agent, was purchased from Sigma Aldrich (St. Louis, MO, USA).

2.2. Nanoparticle preparation

The nanoparticle suspensions were prepared using a nanoprecipitation and solvent displacement method, similar to that employed by Fessi et al.[26] In this method, the copolymers are dissolved at room temperature in a solvent which is thermodynamically efficient for both blocks, in this case Acetone, followed by the slow and progressive addition of a solvent selective for one block (in this case Milli-Q water was used as the solvent selective for the PEO block).[27] The rate of addition of the selective solvent and stirring speed were defined after several experiments. The PLA, which is the hydrophobic block, was organized so as to minimize contact with the solvent (Milli-Q water), promoting the formation of well-defined nanostructures. The best conditions to promote the formation of well-defined and homogeneous (absence of aggregates) nanoparticles, with a low polydispersity index, were the addition of the selective solvent at 7.63 mL h^{-1} (using a syringe of 2 mL) and a stirring rate of 2500 rpm.

For the encapsulation of the essential oil, the preparation procedure was the same as that used for the nanoparticles except for the presence of lavender oil in the organic phase.

2.3. Static (SLS) and dynamic (DLS) light scattering

The technique of dynamic light scattering was used to analyze the morphology of the nanoparticles and the interactions between them and these data were correlated with the same dimensions in aqueous suspensions, based on the temporal fluctuations in the scattered light, which generates data on the dynamics of particles in solution.[28] The experiments were performed using an ALV/CG6-8F goniometer equipped with a 35 mW red helium−neon linearly polarized laser (λ = 632.8 nm) and an ALV/LSE-5004 multiple tau digital correlator with an initial sampling time of 125 ns.[29] The samples were kept at 25 °C. The accessible scattering angle of the equipment ranges from 12 to 155°. After filtration through a 0.45 μM cellulose acetate filter, all samples were systematically studied at 90°, 60º and 120º and some of them were studied at

different scattering angles (varying from 40 to 140°), with a stepwise increase of 10°. The solutions were loaded into 10-mm-diameter glass cells. The minimum sample volume required for the experiment was 0.8 mL. The data were acquired with the ALV correlator control software and the counting time for each sample was typically 300 s. The distributions of the relaxation times, A(t), were obtained using CONTIN analysis applied to the autocorrelation function, C(q, t).[30] The relaxation time, which is denoted as τ, corresponds to the local maxima of the distributions A(t) and the relaxation frequencies (Γ) are equal to 1/τ,[31] while q is the modulus of the scattering vector defined as in with λ being the wavelength of the incident laser beam, n the refractive index of the pure solvent (1.33 for water) and θ the scattering angle (equation 1).[32]

$$q = \frac{4\pi n}{\lambda}\sin\left(\frac{\theta}{2}\right) \quad (1)$$

The hydrodynamic radius (R_H) (or diameter, $2R_H$) was calculated from the Stokes−Einstein equation given in equation 2.

$$R_H = \frac{k_B T}{6\pi\eta D} \quad (2)$$

Where k_B is the Boltzmann constant (in J/K), T is the temperature of the sample (in K), D is the diffusion coefficient and n is the viscosity of the pure solvent (water in this case), (g = 0.89 cP at 25 °C).[33] The radius of gyration (Rg) was calculated from the elastic part (I(q)) of the scattering intensity using the Guinier approximation as follows, where I is the scattering intensity and I_0 is the scattering intensity at q = 0 (equation 3).

$$\ln I = \ln I_0 - \frac{1}{3}q^2 Rg^2 \quad (3)$$

The relationship between Rg and R_H gives the parameter ρ which represents the morphology.

2.4. Transmission electron microscopy (TEM) and atomic force microscopy (AFM)

The morphology of the nanoparticles was evaluated by transmission electron microscopy (TEM) using a CM200 Philips (FEI Company, Hillsboro, USA) microscope at an accelerating voltage of 80 kV. For the analysis, after appropriate dilution in Milli-Q water, 7 µL of an aqueous micellar solution was dropped onto a glow-discharged carbon-coated copper grid. Before the drying process, 7 µL of a 2% (w/v) uranyl acetate negative stain was added. After a few minutes, the excess liquid was blotted with filter paper and the grid was allowed to dry. Images were recorded on Kodak SO163 film and the negatives were scanned off-line using a Kodak Mega plus CCD camera.

The morphology of the samples was also characterized using atomic force microscopy (AFM). The AFM measurements were performed in air using the tapping mode (PicoPlus) at the NanoBio Laboratory of the Joseph Fourier University of Grenoble, France. For the tapping mode a silicon probe was used, with an oscillating frequency of 190 kHz. The scanning area was 1–10 µm^2 with a force constant of 48 N/m and a tip height of 14 µm. The images were treated using Gwyddion 2.31 software to analyze the images and determine the nanoparticle size.

2.5. Zeta potential measurement

Zeta potential data were obtained by laser-doppler anemometry using a Zetasizer Nano Series System (Malvern Instruments, Worcestershire, UK). Samples of the nanoparticles were placed in the electrophoretic cell and for the measurements a potential of ± 150 mV was established. The ζ potential values were calculated as the average of three determinations of the electrophoretic mobility values using Smoluchowski's equation.

2.6. Nanoparticle tracking analysis (NTA)

Nanoparticle tracking analysis (NTA) was performed using an LM10 System digital microscope (Malvern Instruments Ltd., Worcestershire, UK). Samples were filtered through a 0.45 mm cellulose acetate filter and introduced into the chamber using a syringe. Video images of the particle movement under Brownian motion were analyzed using the NTA analytical software version 2.1. The measurements were made at room temperature and each video clip was captured over 60 s.

2.7. UV-visible spectroscopy

This technique was used to calculate the encapsulation efficiency and the amount of active agent released. The absorbance of the lavender essential oil by the nanoparticles was analyzed at a wavenumber range of 210-250 nm[34] using a double beam spectrophotometer (CARY 50, Varian).

The analysis of the active agent release profile associated with the nanoparticles was performed using a system with donor (1 mL) and acceptor (100 mL) compartments separated by a cellulose membrane with a pore molecular exclusion of 3.500 Da and with continuous stirring at 37 °C.[35,36] Aliquots (1 mL) were collected from the acceptor compartment at intervals of 2-1800 min and evaluated by UV-Vis spectroscopy at a wavenumber range of 210-250 nm. The aliquots removed were immediately replaced with an equal amount of water to keep a constant volume.

3. Results and Discussion

3.1. Preparation of nanoparticle suspensions

The nanoparticles based on PEO-*b*-PLA block copolymers were successfully prepared by the nanoprecipitation method, as described in Section 2.2. Two block copolymers, PEO_{5KDa}-*b*-$PLA_{4.5KDa}$ and PEO_{5KDa}-*b*-PLA_{10KDa}, were used to prepare nanoparticles with and without lavender oil (LO) incorporated. In the processes of micelle formation in water the hydrophilic PEO block has a tendency to form the superficial coating of the nanoparticles and the hydrophobic PLA part forms the core. This hydrophobic core is an ideal environment for the encapsulation of hydrophobic active agents, while the block in contact with the solvent promotes the stabilization of the interface between the hydrophobic core and the external environment. Images of the suspensions before and after the micelle formation are shown in Figure 1. The Figure 1A corresponds to the solution of copolymer PEO_{5KDa}-*b*-$PLA_{4.5KDa}$ and lavender oil in acetone and the Figure 1B corresponds to the nanoparticle suspension with encapsulated lavender oil. The Figure 1C corresponds to the solution of copolymer PEO_{5KDa}-*b*-PLA_{10KDa} and lavender oil in acetone and 1D is the nanoparticle suspension.For both systems studied, the best conditions for the obtaining stable nanoparticles were: copolymer concentration of 4 mg mL^{-1}; addition of 7.63 mL h^{-1} of water; 10% of lavender oil to the copolymer solution; stirring rate of 2500 rpm; and acetone as an organic solvent. Under these conditions the nanoparticles were stable for up to 23 days.

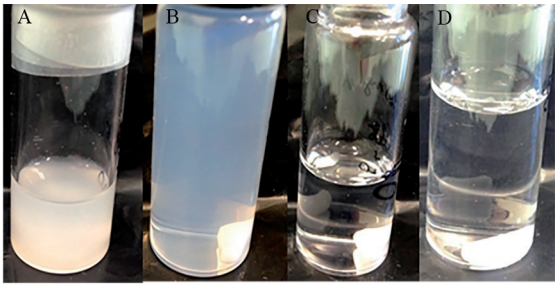

Figure 1: A and C: Solution of copolymer and lavender oil in organic solvent (acetone); B and D: nanoparticle suspension with encapsulated lavender oil.

The size distribution and polydispersity of the nanoparticle suspensions were evaluated considering the angular dependence associated with the light scattering intensity. Considering that the nanoparticle suspensions are in permanent movement, the fluctuation intensity of the scattered light is directly related to Brownian movement. The dynamic light scattering (DLS) technique was used to analyze this movement and correlate it with the dimensions of the nanoparticles in aqueous suspension.[28] The autocorrelation functions ($g^{(2)}$-1) and the relaxation time distribution at a scattering angle of 90° at 25 °C obtained for the two systems studied are shown in Figure 2.

The relaxation time distribution obtained from the self-assembled PEO-*b*-PLA at different copolymer concentrations showed the presence of two micellar populations for samples containing copolymer alone and for the sample PEO_{5KDa}-*b*-PLA_{10KDa} containing oil, where the first (fast relaxation mode) corresponds to the LCMs and the second (slow relaxation mode) probably corresponds to the irregular micellar aggregates formed through the dynamic interaction between the copolymer chains (Figure 2). The dynamic nature of these interactions was confirmed since the micellar aggregates were detected immediately after filtration with a cellulose acetate filter with a pore size of 0.45 μm. The low zeta potential values of the copolymers (close to zero) explain their trend toward the formation of aggregates in solution. The fact that the second peak, appearing in the slow relaxation mode, has a larger area than the first peak (fast relaxation mode) indicates that the quantity of sizes of micellar nanoparticles present are not the same.

It should be noted that the light scattering intensity is proportional to the concentration of the nanoparticles multiplied by their molar mass, according to the Rayleigh scattering of spherical particles. The DLS technique is much more sensitive to the presence of large aggregates than small micellar nanoparticles.[17]

The hydrodynamic radius for the two systems determined via the Stokes-Einstein equation (equation 2) and considering the fast and slow relaxation modes are shown in Table 1.

Analyzing at Table 1 and Figure 2, it is observed that empty micelles of the PEO_{5KDa}-*b*-$PLA_{4.5KDa}$ system had hydrodynamic radii of 65 nm (slow mode) and 18 nm (fast mode). In the presence of 10% lavender oil the hydrodynamic radius increased to 75 nm (only a slow relaxation mode occurred). For the PEO_{5KDa}-*b*-PLA_{10KDa} system the values were 18 nm (slow mode) and 4 nm (fast mode) for empty micelles. With 10% lavender oil the hydrodynamic radius increased to 23 nm and 10 nm, respectively.

The above results indicate that the size and polydispersity index of the PEO-*b*-PLA nanoparticles with and without lavender oil are consistent with colloidal suspensions.[37] Also, it was observed that the presence of lavender oil affected the nanoparticle size (R_H increased), confirming the encapsulation process. The nanoparticle size decreased with an increase in the PLA content of the copolymer.[38] These effects can be explained considering two different situations: i) small nanoparticles are initially obtained, which by aggregation can generate agglomerates,[39] as in the case of PEO_{5KDa}-*b*-$PLA_{4.5KDa}$; and ii) the PEO chains in aqueous solution can form large thermodynamic reversible complexes, increasing the size.[38] In fact, the nanoparticles obtained from the PEO_{5KDa}-*b*-$PLA_{4.5KDa}$ copolymer (lower PLA content) were significantly larger than those obtained from the PEO_{5KDa}-*b*-PLA_{10KDa} system, suggesting a dependence on the PEO.[33]

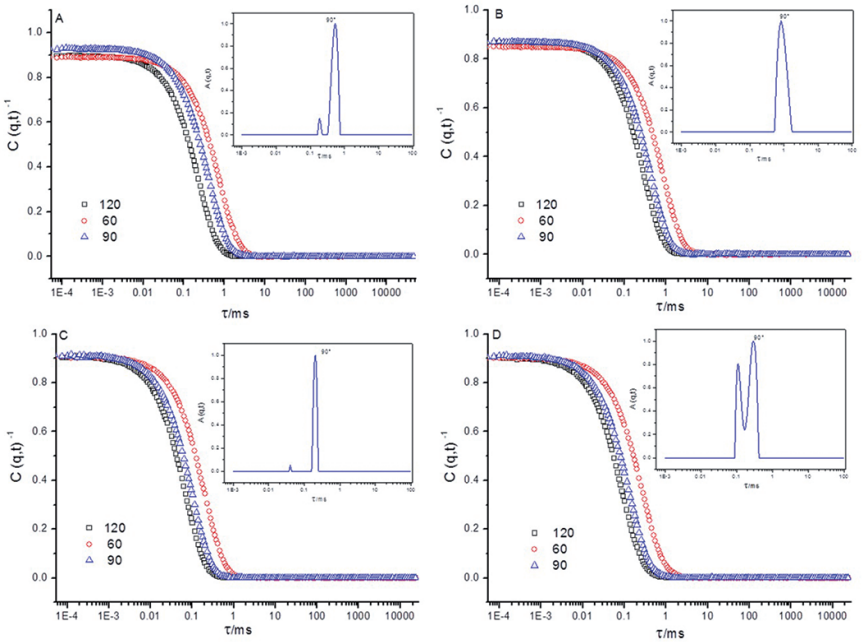

Figure 2: Correlation function at 90°, 60° and 120° and decay time distribution obtained at a 90° scattering angle for: (A) PEO_{5KDa}-*b*-$PLA_{4.5KDa}$ filtered through a 0.45 µm membrane; (B) PEO_{5KDa}-*b*-$PLA_{4.5KDa}$ containing 10% LO filtered through a 0.45 µm membrane; (C) PEO_{5KDa}-*b*-PLA_{10KDa} filtered through a 0.45 µm membrane; and (D) PEO_{5KDa}-*b*-PLA_{10KDa} containing 10% LO filtered through a 0.45 µm membrane.

Table 1: Hydrodynamic radius (R_H) values for PEO-*b*-PLA self-assembled systems with and without lavender oil (LO).

	RH			
Copolymer sample	Empty NP		NP with 10% of LO	
	R_{H1}	R_{H2}	R_{H1}	R_{H2}
PEO_{5KDa}-*b*-$PLA_{4.5KDa}$	18	66	-	78
PEO_{5KDa}-*b*-PLA_{10KDa}	4	18	10	23

A bimodal distribution was observed for PEO_{5KDa}-*b*-PLA_{10KDa} nanoparticles with lavender oil, suggesting the formation of aggregates in this system. The polydispersity index slightly increased with the presence of lavender oil, from 0.27 to 0.34 and 0.30 to 0.32 for the PEO_{5KDa}-*b*-$PLA_{4.5KDa}$ and PEO_{5KDa}-*b*-PLA_{10KDa} systems, respectively. In general, parameters such as nanoparticle size, polydispersity index and zeta potential are related to the suspension stability. In our case, the polydispersity index was close to 0.3 for both systems studied, suggesting good stability under the preparation conditions.[40] The zeta potential is also a parameter that can influence the particle stability in suspension based on the electrostatic repulsion and its measurement also provides information regarding the dominant block on the particle surface. For the samples evaluated in this study the zeta potential was close to neutral (data not shown), suggesting the presence of PEO (non-ionic) on the surface of the nanoparticles.

3. 2. Microscopy evaluation

The morphology of the nanoparticles obtained was evaluated through TEM and AFM. For both systems studied spherical nanoparticles were obtained,[41,8] as exemplified in Figure 3 (TEM) and Figure 4 (AFM). The TEM micrographs showed slightly smaller sizes for the nanoparticles in comparison with the DLS results. This difference is associated with the natural dehydration process during the sample preparation in the case of the TEM measurements. The TEM micrographs, similarly to the DLS results, also showed an increase in the average radius of the nanoparticles with the addition of lavender oil (Figures 3B and 3D). For example, the nanoparticles obtained with the copolymer PEO_{5KDa}-*b*-PLA_{10KDa} showed average diameters of 50 nm and 56 nm without and with 10% LO, respectively.

In the case of AFM, compact and spherical nanoparticles were also observed. The diameters of the nanoparticles obtained from the copolymer PEO_{5KDa}-*b*-$PLA_{4.5KDa}$ without and

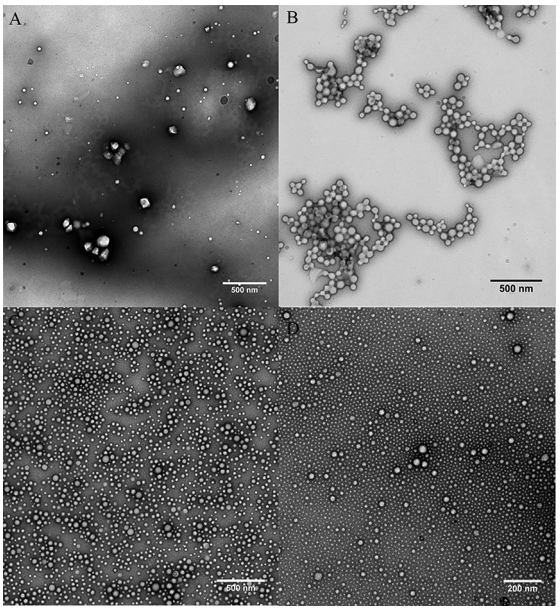

Figure 3: Transmission electron micrographs of the nanoparticles after filtration through 0.45 µm membranes and their histograms for: (A) PEO_{5KDa}-*b*-$PLA_{4.5KDa}$; (B) PEO_{5KDa}-*b*-$PLA_{4.5KDa}$ containing 10% lavender essential oil; (C) PEO_{5KDa}-*b*-PLA_{10KDa}; and (D) PEO_{5KDa}-*b*-PLA_{10KDa} containing 10% lavender essential oil.

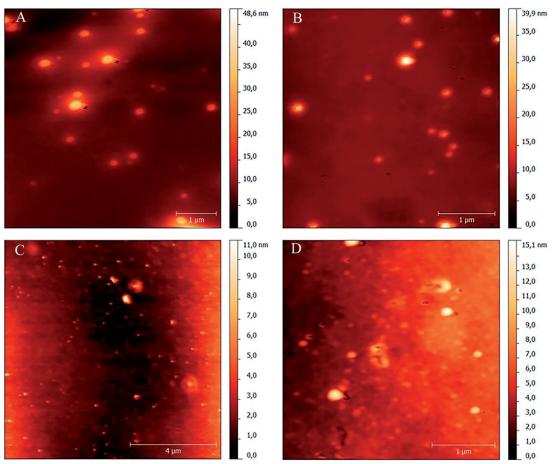

Figure 4: AFM images of the topography of self-assembled nanoparticles after filtration through 0.45 µm membranes: (A) PEO_{5KDa}-*b*-$PLA_{4.5KDa}$; (B) PEO_{5KDa}-*b*-$PLA_{4.5KDa}$ containing 10% lavender essential oil; (C) PEO_{5KDa}-*b*-PLA_{10KDa}; (D) PEO_{5KDa}-*b*-PLA_{10KDa} containing 10% lavender essential oil.

with 10% LO were in the range of 40-80 nm and 60-80 nm, respectively (Figures 4A and 4B), while the corresponding values for nanoparticles of PEO_{5KDa}-*b*-PLA_{10KDa} were 15 nm (4C) and 20 nm (4D), respectively. Although the size could be estimated from the AFM images it was not possible to define with good accuracy the nanoparticle morphology. An exception was the PEO_{5KDa}-*b*-PLA_{10KDa} copolymer, for which a more regular and defined spherical morphology was observed, similarly to results reported in the literature.[11]

3.3. Static and dynamic light scattering

Figure 5 shows the typical variation in the measured angular frequency Γ as a function of q^2, indicating a diffusive scattering behavior for the PEO_{5KDa}-*b*-$PLA_{4.5KDa}$ and PEO_{5KDa}-*b*-PLA_{10KDa} nanoparticles with or without lavender oil, confirming the formation of spherical nanoparticles. The radius of gyration (Rg) was calculated based on the Guinier model, more specifically, the slope of the straight line obtained using Equation 1. This approach is often used to determine the particle Rg value, and is valid only when $qRg < 1$. All samples showed a similar behavior, indicating the same nanoparticle morphology, i.e., the formation of spherical micelles.

The Rg and R_H values for the systems studied are summarized in Table 2. The ratio between Rg and R_H provides the anisotropic degree (ρ), which is associated with the morphology of the nanoparticles. According to Table 1, the ρ value ranged between 0.70 and 1.14, suggesting the formation of spherical nanoparticles, which is in agreement with the morphologies observed by TEM and AFM.

The results presented in Table 2 also show that the size (hydrodynamic diameter) and polydispersity of the PEO-*b*-PLA nanoparticles with or without lavender oil are consistent with colloidal suspensions. The hydrodynamic radius increased for nanoparticles containing lavender oil, suggesting, in agreement with the UV results, that the active agent was effectively encapsulated (see the last section of the results). The R_H of nanoparticles obtained from PEO_{5KDa}-*b*-$PLA_{4.5KDa}$ increased from 65 nm to 75 nm[42,43] with 10% LO and from 18 nm to 23 nm for the PEO_{5KDa}-*b*-PLA_{10KDa} system.[44]

By zeta potential measurements was observed that the nanoparticles suspensions were stable up to 23 days. After this period, both polydispersity and nanoparticles size increased, suggesting the formation of aggregates. In the present case, the PLA block promotes a steric stabilization of the nanoparticle suspension. As previously discussed in the literature, the diblock copolymer chains are attached to the surface of the nanoparticles via hydrophobic interactions with the PLA block whereas the hydrophilic PEO blocks and the solvation process in the aqueous medium promote a steric barrier.[45,46]

The hydrodynamic radius determined by DLS were compared with those obtained from the zeta potential and SLS experiments. The results shown in Table 2 indicate a good similarity and a clear tendency toward increased particle size with decreasing molecular weight of PLA block was observed.[15]

3.4. NTA experiments

In order to confirm the results obtained by DLS, suggesting that the nanoparticles obtained have low polydispersity, the samples were analyzed by nanoparticle tracking analysis

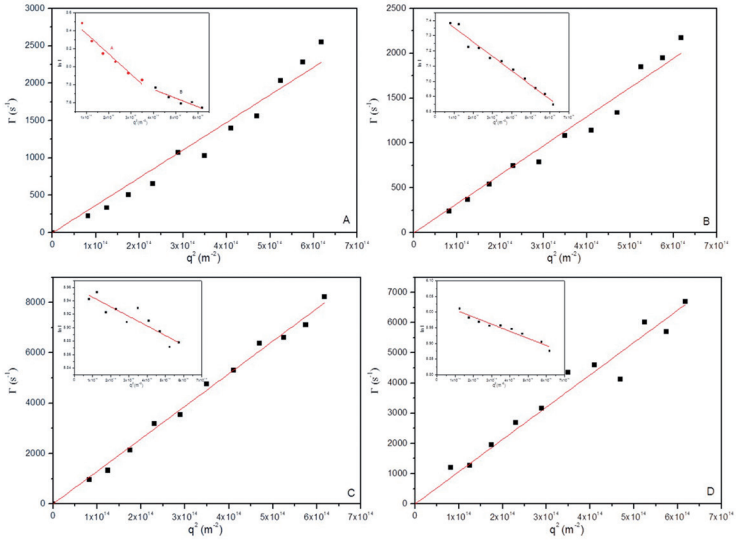

Figure 5: Dependence of the relaxation frequency (1/τ) on the squared wave vector modulus (q^2) of the aqueous suspensions of (A) PEO_{5KDa}-*b*-$PLA_{4.5KDa}$ filtered through a 0.45 µm membrane; (B) PEO_{5KDa}-*b*-$PLA_{4.5KDa}$ containing 10% lavender essential oil filtered through a 0.45 µm membrane; (C) PEO_{5KDa}-*b*-PLA_{10KDa} filtered through a 0.45 µm membrane; and (D) PEO_{5KDa}-*b*-PLA_{10KDa} containing 10% lavender essential oil filtered through a 0.45 µm membrane.

Table 2: Hydrodynamic radius determined by DLS and zeta potential experiments, hydration radius (SLS), polydispersity and anisotropic degree.

Systems	R_H (nm, DLS)	R_H (nm, ZP)*	R_g (nm)	PDI	*P*
PEO_{5K}-*b*-$PLA_{4.5K}$	66	79	65	0.27	0.97
PEO_{5K}-*b*-$PLA_{4.5K}$ + LO	78	78	53	0.34	0.70
PEO_{5K}-*b*-PLA_{10K}	18	26	20	0.30	1.09
PEO_{5K}-*b*-PLA_{10K} + LO	23	28	26	0.32	1.14

*Particle size is given as the mean hydrodynamic diameter of the particles calculated from the intensity of the scattered light (Z-average size) using the Zetasizer software version 7.01.

(NTA),[36] a technique based on laser illumination microscopy, which allows the real-time analysis of the Brownian motion of nanoparticles using a charge-coupled device (CCD) camera. In this method, nanoparticles in a liquid environment are visualized and tracked individually using image analysis software that deduces the diffusion coefficient of each particle and allows the determination of its hydrodynamic radius.[47] This analysis method is considered to complement dynamic light scattering since it gives the number average diameter. The nanoparticle size distribution, with the corresponding video frames and three-dimensional graphs (size vs. intensity vs. concentration), for the nanoparticle samples obtained from the copolymer PEO_{5KDa}-*b*-$PLA_{4.5KDa}$, are shown in Figure 6. A relatively narrow distribution can be observed for all formulations, showing good agreement with the DLS results. However, the average diameters obtained by NTA for samples of PEO_{5KDa}-*b*-PLA_{10KDa} were higher than those obtained by DLS, since NTA lacks sensitivity for nanoparticles very smaller. Average diameters of 125 nm, for empty nanoparticles, and 80 nm for nanoparticles containing lavender essential oil, were obtained by NTA, which are slightly larger compared with the results obtained by DLS. According to Filipe et al.,[48] this difference can be explained considering that the size distributions obtained by DLS are weight distributions, whereas those obtained by NTA relate to number distributions. Thus, the size distribution obtained by NTA indicates larger sizes compared to the DLS results, due to the contribution of some large particles to the overall dispersion.[39]

3.5. Encapsulation and in vitro release of essential oil

The percentage of lavender oil encapsulated in the nanoparticles was determined by the ultrafiltration/centrifugation method. Nanoparticles containing lavender oil were centrifuged in Amicon-Ultra-0.5 cellulose ultrafiltration filters with a molecular exclusion regenerated portion of 30 KDa (Microcon - Millipore) at 10.000 rpm for 30 min and the filtrate was quantified by UV-Vis spectroscopy at a wavenumber range of 210-250 nm. The amount encapsulated was determined as the difference between the lavender oil concentration in the filtrate and the total concentration (100%) which was initially present in the nanoparticle suspension.[29] As shown

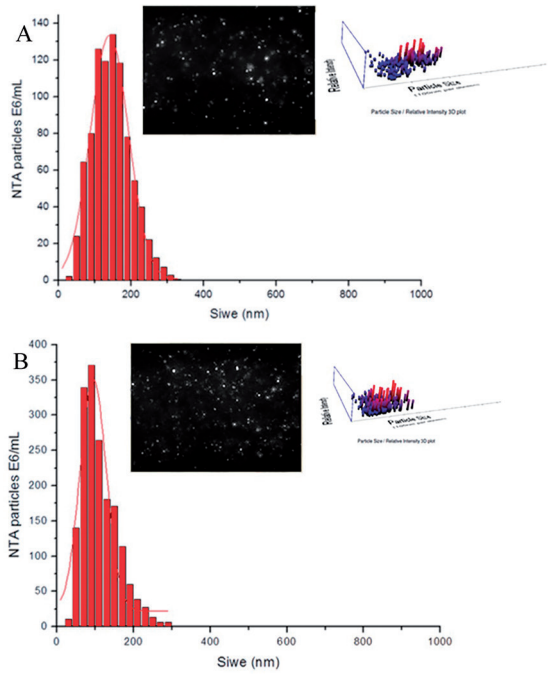

Figure 6: Size distributions obtained from NTA measurements with the corresponding captured images from NTA video and 3D graph size vs. intensity vs. concentration obtained for: (A) PEO_{5KDa}-*b*-$PLA_{4.5KDa}$ filtered through a 0.45 µm membrane; and (B) PEO_{5KDa}-*b*-$PLA_{4.5KDa}$ containing 10% lavender essential oil filtered through a 0.45 µm membrane. The NTA videos obtained are available as supplementary data.

Table 3: Entrapment efficiency and essential oil quantification of the nanoparticle suspensions.

Sample	Essential Oil Content (mg/mL)	EE (%)	Recovery (%)
PEO_{5K} –$PLA_{4.5K}$	0.4	73	85
PEO_{5K} –PLA_{10K}	0.4	75	93

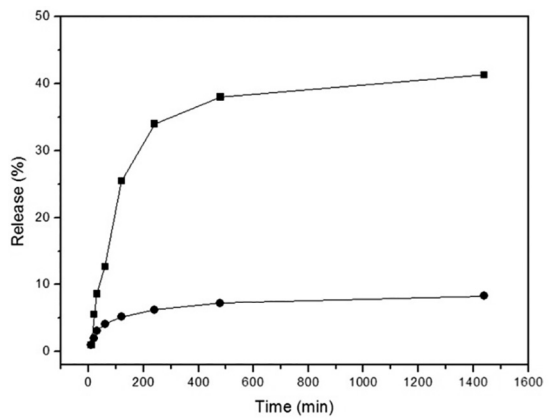

Figure 7: Releasing profile of nanoparticles containing 10% lavender essential oil: (■)PEO_{5KDa}-*b*-PLA_{10KDa}; (●) PEO_{5KDa}-*b*-$PLA_{4.5KDa}$.

in Table 3, the values for the encapsulation efficiency of the lavender oil were 73 and 75% for the PEO_{5KDa}-*b*-$PLA_{4.5KDa}$ and PEO_{5KDa}-*b*-PLA_{10KDa} systems, respectively. These results are in agreement with those obtained by Silva de Melo,[29] who reported an EE value of 73% for the encapsulation of benzocaine in PLA nanoparticles.

For the lavender oil in a concentration of 0.4 mg/mL the recovery percentages were 85 and 93% for nanoparticles obtained from the PEO_{5KDa}-*b*-$PLA_{4.5KDa}$ and PEO_{5KDa}-*b*-PLA_{10KDa} systems, respectively. This result suggests that a very low amount of lavender oil was located on the surface or more external part of the nanoparticles and that most of the oil was entrapped in the nanoparticles.

The preliminary results concerning the percentages of the amount of lavender oil released versus time are shown in Figure 7. The results showed that the release of lavender essential oil from PEO_{5KDa}-*b*-$PLA_{4.5KDa}$ nanoparticles was only 5% and this percentage remained the same for 24h of releasing process. However, a different behavior was observed for PEO_{5KDa}-*b*-PLA_{10KDa} nanoparticles, in which the released amount achieved 40%. As observed, the releasing percentage was dependent on the PLA molecular weight, increasing with the amount of PLA in the block copolymer. As we previously discussed, the size of the nanoparticles obtained from the PEO_{5KDa}-*b*-PLA_{10KDa} system were significantly smaller than those obtained from the PEO_{5KDa}-*b*-$PLA_{4.5KDa}$ copolymer. Apparently, small nanoparticles favored the diffusion process, increasing in consequence, the amount of lavender oil released in this system.

4. Conclusions

Suspensions of nanoparticles were obtained by the nanoprecipitation method and controlled self-assembly of the PEO-*b*-PLA copolymer. The preparation technique used led to the formation of spherical nanoparticles of PEO-*b*-PLA with low polydispersity. The hydrodynamic radius of the nanoparticles were in the range of 10 to 75 nm and a dependence on the size of the PLA block was observed. The encapsulation efficiency determined by UV-VIS spectroscopy was in the range of 70-75%; however, the in vitro release suggests that the polymeric system used in this study is able to control and retard the oil release. Considering that nanostructured systems can encapsulate poorly-water soluble active agents, such as essential oils, we may conclude that the nanoparticles obtained from PEO-*b*-PLA copolymers were effective in incorporating the lavender oil. Studies associated with the antibacterial effect of the lavender oil encapsulated in PEO-*b*-PLA nanoparticles are still in progress.

5. Acknowledgements

The authors acknowledge financial support from Institut Carnot PolyNat, CERMAV, CNRS, CAPES, CNPq and the Federal University of Santa Catarina (UFSC).

6. References

1. Giacomelli C, Schmidt V, Aissou K, Borsali R. Block copolymer systems: from single chain to self-assembled nanostructures. *Langmuir*. 2010;26(20):15734-15744. http://dx.doi.org/10.1021/la100641j

2. Lavasanifar A, Samuel J, Kwon GS. Poly(ethylene oxide)-*block*-poly(L-amino acid) micelles for drug delivery. *Advanced Drug Delivery Reviews*. 2002;54(2):169-190. http://dx.doi.org/10.1016/S0169-409X(02)00015-7

3. Vrignaud S, Benoit JP, Saulnier P. Strategies for the nanoencapsulation of hydrophilic molecules in polymer-based nanoparticles. *Biomaterials*. 2011;32(33):8593-8604. http://dx.doi.org/10.1016/j.biomaterials.2011.07.057

4. Zhang L, Chan JM, Gu FX, Rhee JW, Wang AZ, Radovic-Moreno AF, et al. Self-assembled lipid--polymer hybrid nanoparticles: a robust drug delivery platform. *ACS Nano*. 2008;2(8):1696-1702. http://dx.doi.org/10.1021/nn800275r

5. Donsì F, Sessa M, Ferrari G. Nanoencapsulation of essential oils to enhance their antimicrobial activity in foods. *Journal of Biotechnology*. 2010;150 Suppl:S576. http://dx.doi.org/10.1016/j.jbiotec.2010.08.175

6. Mosqueira VCF, Legrand P, Gulik A, Bourdon O, Gref R, Labarre D, et al. Relationship between complement activation, cellular uptake and surface physicochemical aspects of novel PEG-modified nanocapsules. *Biomaterials*. 2001;22(22):2967-2979. http://dx.doi.org/10.1016/S0142-9612(01)00043-6

7. Drumond WS, Wang SH, Mothé CG. Síntese e caracterização do copolímero poli (ácido lático-*b*-glicol etilênico). *Polímeros*. 2004;14(2):74-79. http://dx.doi.org/10.1590/S0104-14282004000200009

8. Loch Neckel G, Lemos-Senna E. Preparação e caracterização de nanocápsulas contendo camptotecina a partir do ácido poli (D,L-lático) e de copolímeros diblocos do ácido Poli (D,L-lático) e polietilenoglicol. *Acta Farmacéutica Bonaerense*. 2005;24(4):504-511.

9. Lasprilla AJR, Martinez GAR, Lunelli BH, Jardini AL, Maciel Filho R. Poly-lactic acid synthesis for application in biomedical devices – A review. *Biotechnology Advances*. 2012;30(1):321-328. http://dx.doi.org/10.1016/j.biotechadv.2011.06.019

10. Heald CR, Stolnik S, de Matteis C, Garnett MC, Illum L, Davis SS, et al. Self-consistent field modelling of poly(lactic acid)–poly(ethylene glycol) particles. *Colloids and Surfaces A: Physicochemical and Engineering Aspects*. 2001;179(1):79-91. http://dx.doi.org/10.1016/S0927-7757(00)00729-9

11. Chorny M, Fishbein I, Danenberg HD, Golomb G. Lipophilic drug loaded nanospheres prepared by nanoprecipitation: effect of formulation variables on size, drug recovery and release kinetics. *Journal of Controlled Release*. 2002;83(3):389-400. http://dx.doi.org/10.1016/S0168-3659(02)00211-0

12. Dai R, Lim LT. Release of allyl isothiocyanate from mustard seed meal powder entrapped in electrospun PLA–PEO nonwovens. *Food Research International*. 2015;77(3):467-475. http://dx.doi.org/10.1016/j.foodres.2015.08.029

13. Jie P, Venkatraman SS, Min F, Freddy BYC, Huat GL. Micelle-like nanoparticles of star-branched PEO–PLA copolymers as chemotherapeutic carrier. *Journal of Controlled Release*. 2005;110(1):20-33. http://dx.doi.org/10.1016/j.jconrel.2005.09.011

14. Cohn D, Hotovely-Salomon A. Biodegradable multiblock PEO/PLA thermoplastic elastomers: molecular design and properties. *Polymer*. 2005;46(7):2068-2075. http://dx.doi.org/10.1016/j.polymer.2005.01.012

15. Ramot Y, Zada MH, Domb AJ, Nyska A. Biocompatibility and safety of PLA and its copolymers. *Advanced Drug Delivery Reviews*. 2016;pii: S0169-409X(16)30098-9. http://dx.doi.org/10.1016/j.addr.2016.03.012.

16. Ahmed F, Discher DE. Self-porating polymersomes of PEG–PLA and PEG–PCL: hydrolysis-triggered controlled release vesicles. *Journal of Controlled Release*. 2004;96(1):37-53. http://dx.doi.org/10.1016/j.jconrel.2003.12.021

17. Riley T, Stolnik S, Heald CR, Xiong CD, Garnett MC, Illum L, et al. Physicochemical Evaluation of Nanoparticles Assembled from Poly(lactic acid)-Poly(ethylene glycol) (PLA-PEG) Block Copolymers as Drug Delivery Vehicles. *Langmuir*. 2001;17(11):3168-3174. http://dx.doi.org/10.1021/la001226i

18. Rodríguez J, Martín MJ, Ruiz MA, Clares B. Current encapsulation strategies for bioactive oils: From alimentary to pharmaceutical perspectives. *Food Research International*. 2016;83:41-59. http://dx.doi.org/10.1016/j.foodres.2016.01.032

19. Xiao Z, Liu W, Zhu G, Zhou R, Niu Y. Production and characterization of multinuclear microcapsules encapsulating lavender oil by complex coacervation. *Flavour and Fragrance Journal*. 2014;29(3):166-172. http://dx.doi.org/10.1002/ffj.3192

20. Donsì F, Annunziata M, Sessa M, Ferrari G. Nanoencapsulation of essential oils to enhance their antimicrobial activity in foods. *LWT - Food Science and Technology*. 2011;44(9):1908-1914. http://dx.doi.org/10.1016/j.lwt.2011.03.003

21. Gavini E, Sanna V, Sharma R, Juliano C, Usai M, Marchetti M, et al. Solid lipid microparticles (SLM) containing juniper oil as anti-acne topical carriers: preliminary studies. *Pharmaceutical Development and Technology*. 2005;10(4):479-487. http://dx.doi.org/10.1080/10837450500299727

22. Gaysinsky S, Davidson PM, Bruce BD, Weiss J. Growth inhibition of *Escherichia coli* O157: H7 and Listeria monocytogenes by carvacrol and eugenol encapsulated in surfactant micelles. *Journal of Food Protection*. 2005;68(12):2559-2566. http://dx.doi.org/10.4315/0362-028X.JFP-08-403

23. Kim HM, Cho SH. Lavender oil inhibits immediate-type allergic reaction in mice and rats. *Journal of Pharmacy and Pharmacology*. 1999;51(2):221-226. http://dx.doi.org/10.1211/0022357991772178

24. Martín A, Varona S, Navarrete A, Cocero MJ. Encapsulation and Co-precipitation Process with Supercritical Fluids: Application with Essential Oils. *The Open Chemical Engineering Journal*. 2010;4:31-41. http://dx.doi.org/10.2174/1874123101004010031

25. Balasubramanian K, Kodam KM. Encapsulation of therapeutic lavender oil in an electrolyte assisted polyacrylonitrile nanofibres for antibacterial applications. *RSC Advances*. 2014;4:54892-54901. http://dx.doi.org/10.1039/c4ra09425e

26. Fessi H, Devissaguet JP, Puisieux F, Thies C, inventors. *Procede de préparation de systèmes colloïdaux dispersibles d´une substance sous forme de nanoparticules*. European Patent 0275796 B1. 1987.

27. Houga C, Giermanska J, Lecommandoux S, Borsali R, Taton D, Gnanou Y, et al. Micelles and Polymersomes Obtained by Self-Assembly of Dextran and Polystyrene Based Block Copolymers. *Biomacromolecules*. 2009;10(1):32-40. http://dx.doi.org/10.1021/bm800778n

28. Schärtl W. *Light Scattering from Polymer Solutions and Nanoparticle Dispersions*. 1st ed. Berlin Heidelberg: Springer-Verlag; 2007. 191 p.

29. Berne BJ, Pecora R. *Dynamic Light Scattering: With Applications to Chemistry, Biology, and Physics*. 2nd ed. Mineola: Dover Publications; 2000.

30. Provencher SW. Inverse problems in polymer characterization: Direct analysis of polydispersity with photon correlation spectroscopy. *Macromolecular Chemistry and Physics*. 1979;180(1): 201-209. http://dx.doi.org/10.1002/macp.1979.021800119.

31. Tammer M, Horsburgh L, Monkman AP, Brown W, Burrows HD. Effect of Chain Rigidity and Effective Conjugation Length on the Structural and Photophysical Properties of Pyridine-Based Luminescent Polymers. *Advanced Functional Materials*. 2002;12(6-7):447-454. http://dx.doi.org/10.1002/1616-3028(20020618)12:6/7

32. Dal Bó AG, Soldi V, Giacomelli FC, Travelet C, Jean B, Pignot-Paintrand I, et al. Self-Assembly of Amphiphilic Glycoconjugates into Lectin-Adhesive Nanoparticles. *Langmuir*. 2012;28(2):1418-1426. http://dx.doi.org/10.1021/la204388h

33. Giacomelli C, Schmidt V, Borsali R. Nanocontainers Formed by Self-Assembly of Poly(ethylene oxide)-*b*-poly(glycerol monomethacrylate)−Drug Conjugates. *Macromolecules*. 2007;40(6):2148-2157. http://dx.doi.org/10.1021/ma062562u

34. Sirvaityte J, Siugzdaite J, Valeika V. Application of Commercial Essential Oils of Eucalyptus and Lavender as Natural Preservative for Leather Tanning Industry. *Revista de Chimie (Bucharest)*. 2011;62(9):884-893.

35. Paavola A, Yliruusi J, Kajimoto Y, Kalso E, Wahlström T, Rosenberg P. Controlled release of lidocaine from injectable gels and efficacy in rat sciatic nerve block. *Pharmaceutical Research*. 1995;12(12):1997-2002. http://dx.doi.org/10.1023/A:1016264527738

36. Silva de Melo NF, Grillo R, Rosa AH, Fraceto LF, Dias Filho NL, de Paula E, et al. Desenvolvimento e caracterização de nanocápsulas de poli (L-lactídeo) contendo benzocaína. *Química Nova*. 2010;33(1):65-69. http://dx.doi.org/10.1590/S0100-40422010000100013

37. Guterres SS, Fessi H, Barrat G, Devissaguet JP, Puisieux F. Poly (DL-lactide) nanocapsules containing diclofenac: I. Formulation and stability study. *International Journal of Pharmaceutics*. 1995;113(1):57-63. http://dx.doi.org/10.1016/0378-5173(94)00177-7

38. Hu Y, Jiang X, Ding Y, Zhang L, Yang C, Zhang J, et al. Preparation and drug release behaviors of nimodipine-loaded poly(caprolactone)–poly(ethylene oxide)–polylactide amphiphilic copolymer nanoparticles. *Biomaterials*. 2003;24(13):2395-2404. http://dx.doi.org/10.1016/S0142-9612(03)00021-8

39. Xu R, Winnik MA, Hallett FR, Riess G, Croucher MD. Light-scattering study of the association behavior of styrene-ethylene oxide block copolymers in aqueous solution. *Macromolecules*. 1991;24(1):87-93. http://dx.doi.org/10.1021/ma00001a014

40. Mohanraj VJ, Chen Y. Nanoparticles – A Review. *Tropical Journal of Pharmaceutical Research*. 2006;5(1):561-573. http://dx.doi.org/10.4314/tjpr.v5i1.14634

41. Liu Z, Jiang M, Kang T, Miao D, Gu G, Song Q, et al. Lactoferrin-modified PEG-co-PCL nanoparticles for enhanced brain delivery of NAP peptide following intranasal administration. *Biomaterials*. 2013;34(15):3870-3881. http://dx.doi.org/10.1016/j.biomaterials.2013.02.003.

42. Muller CR, Bassani VL, Pohlmann AR, Michalowski CB, Petrovick PR, Guterres SS. Preparation and characterization of spray-dried polymeric nanocapsules. *Drug Development and Industrial Pharmacy*. 2000;26(3):343-347. http://dx.doi.org/10.1081/DDC-100100363

43. Schaffazick SR, Pohlmann AR, Freitas LL, Guterres SS. Caracterização e Estudo de Estabilidade de Suspensões de Nanocápsulas e de Nanoesferas Poliméricas Contendo Diclofenaco. *Acta Farmacéutica Bonaerense*. 2002;21(2):99-106.

44. Schaffazick SR, Guterres SS, Freitas LL, Pohlmann AR. Caracterização e estabilidade físico-química de sistemas poliméricos nanoparticulados para administração de fármacos. *Química Nova*. 2003;26(5):726-737. http://dx.doi.org/10.1590/S0100-40422003000500017

45. Santander-Ortega MJ, Csaba N, Alonso MJ, Ortega-Vinuesa JL, Bastos-González D. Stability and physicochemical characteristics of PLGA, PLGA:poloxamer and PLGA:poloxamine blend nanoparticles: A comparative study. *Colloids and Surfaces A: Physicochemical and Engineering Aspects*. 2007;296(1-3):132-140. http://dx.doi.org/10.1016/j.colsurfa.2006.09.036

46. Mazzarino L, Travelet C, Murillo SO, Otsuka I, Pignot-Paintrand I, Senna EL, et al. Elaboration of chitosan-coated nanoparticles loaded with curcumin for mucoadhesive applications. *Journal of Colloid and Interface Science*. 2012;370(1):58-66. http://dx.doi.org/10.1016/j.jcis.2011.12.063.

47. Malvern instrument - NanoSight range. Available from: <http://www.nanosight.com>. Access in: 6/5/2014.

48. Filipe V, Hawe A, Jiskoot W. Critical Evaluation of Nanoparticle Tracking Analysis (NTA) by NanoSight for the measurement of nanoparticles and protein aggregates. *Pharmaceutical Research*. 2010;27(5):796-810. http://dx.doi.org/10.1007/s11095-010-0073-2.